

# HELENA: High-Efficiency Learning-based channel Estimation using dual Neural Attention

Miguel Camelo Botero, Esra Aycan Beyazıt, Nina Slamnik-Kriještorac, Johann M. Marquez-Barja  
University of Antwerp - imec, IDLab, Antwerp, Belgium

**Abstract**—Accurate channel estimation is critical for high-performance Orthogonal Frequency-Division Multiplexing systems such as 5G New Radio, particularly under low signal-to-noise ratio and stringent latency constraints. This letter presents HELENA, a compact deep learning model that combines a lightweight convolutional backbone with two efficient attention mechanisms: patch-wise multi-head self-attention for capturing global dependencies and a squeeze-and-excitation block for local feature refinement. Compared to CEViT, a state-of-the-art vision transformer-based estimator, HELENA reduces inference time by 45.0% (0.175 ms vs. 0.318 ms), achieves comparable accuracy (−16.78 dB vs. −17.30 dB), and requires 8× fewer parameters (0.11M vs. 0.88M), demonstrating its suitability for low-latency, real-time deployment.

**Index Terms**—Channel Estimation, 5G-NR, OFDM, Deep Learning, Neural Attention, Neural Network Acceleration.

## I. INTRODUCTION

Accurate estimation of Channel State Information (CSI) is crucial for the effectiveness of Orthogonal Frequency-Division Multiplexing (OFDM)-based wireless communication systems, such as 5G New Radio (5G-NR), as it enables optimal resource allocation, beamforming, and adaptive modulation, all of which directly impact system capacity and reliability. In this context, Channel Estimation (CE) refers to the process of acquiring or predicting CSI using received signals and known reference signals (e.g., pilot symbols). This process entails analyzing how the wireless channel affects transmitted signals using a variety of estimation algorithms. However, traditional methods like Least Squares (LS) and Minimum Mean Square Error (MMSE) suffer from high estimation error in noisy environments (e.g., LS) or incur substantial computational cost and rely on prior channel statistics (e.g., MMSE), limiting their suitability in low Signal-to-Noise Ratio (SNR) or high-mobility scenarios.

To address these challenges, recent research has investigated both model-based and data-driven approaches for improving CE under realistic 5G and beyond conditions. Among model-based techniques, several recent methods have demonstrated competitive performance by leveraging signal structure and auxiliary information, such as pilot-free estimation for high-Doppler Orthogonal Time Frequency Space (OTFS) scenarios [1] and sensing-assisted denoising of LS estimates [2]. In parallel, Deep Learning (DL)-based methods have emerged as powerful tools for enhancing CE by learning complex propagation patterns directly from data. These approaches lay the foundation for Artificial Intelligence (AI)-native physical

layer design [3] and the development of the next generation of intelligent radios [4], which is the focus of this letter.

Architectures such as ChannelNet [5], Enhanced Deep Super-Resolution (EDSR) [6], Attention mechanism and Residual Network (AttRNet) [7], and the more recent Channel Estimator Vision Transformer (CEViT) [8] have demonstrated superior estimation accuracy compared to conventional estimators. However, their high computational complexity limits their deployment in real-time 5G systems, which are constrained by strict latency, power, and hardware budgets [9], [10]. This has led to the development of lightweight architectures such as LS-augmented interpolated Deep Neural Network (LSiDNN) [11], which aim to balance accuracy with computational efficiency.

To address these limitations, we propose **High-Efficiency Learning-based channel Estimation using dual Neural Attention (HELENA)**, a lightweight hybrid DL architecture for pilot-based CE in OFDM systems without interpolation. It balances estimation accuracy and inference time by combining convolutional feature extraction with a dual-attention design: local features are extracted via 2D Convolutional (Conv2D) layers, global dependencies are captured through patch-wise Multi-Head Self-Attention (MHSA), and salient channels are enhanced using a post-attention Squeeze-and-Excitation (SE) block. A linear reconstruction head and residual connection preserve structural information and support convergence, especially under high-SNR conditions. In this letter, we demonstrate that HELENA (i) achieves better accuracy–efficiency trade-offs than several state-of-the-art DL models, (ii) reveals that computational cost does not always correlate with inference time, and (iii) is fully reproducible, with open-source code and dataset made available<sup>1</sup>.

The remainder of the letter is organized as follows. Section II provides the system model. Section III presents the proposed architecture. In Section IV, simulation results are presented. Finally, section V concludes this letter.

## II. PROBLEM STATEMENT

This research considers the downlink Single Input Single Output (SISO) OFDM system model for 5G-NR. In an OFDM system, for the  $k_{th}$  time slot and the  $i_{th}$  subcarrier, the received signal,  $Y_{i,k}$  is defined as follows.

$$Y_{i,k} = H_{i,k}X_{i,k} + Z_{i,k} \quad (1)$$

<sup>1</sup>[https://github.com/miguelhdo/HELENA\\_Channel\\_Estimation](https://github.com/miguelhdo/HELENA_Channel_Estimation)

where  $X_{i,k}$  is the transmitted OFDM signal and  $Z_{i,k}$  represents Additive White Gaussian Noise (AWGN) with variance  $\sigma^2$ . The considered OFDM subframe size is  $N_S \times N_D$ . The slot index  $k$  range is given as  $[0, N_D - 1]$ , and the subcarrier index  $i$  is given as  $[0, N_S - 1]$ .  $H_{i,k}$  represents the  $(i, k)$  element of the channel matrix  $\mathbf{H} \in \mathbb{C}^{N_S \times N_D}$ .

In practical OFDM systems, the channel matrix  $\mathbf{H}$  is unknown at the receiver and must be estimated from a limited set of pilot subcarriers, resulting in an underdetermined problem. Classical methods such as LS and MMSE [12] rely on pilot-based interpolation [13] to reconstruct the full channel, but each has drawbacks. While LS is computationally efficient, it is sensitive to noise. MMSE provides higher accuracy by using prior channel statistics but is computationally intensive and difficult to implement in dynamic environments. To address these limitations, recent approaches reformulate CE as a Super-resolution (SR) problem. The objective is to reconstruct an accurate channel response  $\hat{\mathbf{H}}$  from sparse pilot observations  $\mathbf{H}_p$ , modeled as:

$$\hat{\mathbf{H}} = f_{\Theta}(\mathbf{H}_{LR}), \quad (2)$$

where  $f_{\Theta}$  represents a DL model parameterized by  $\Theta$ , designed to learn complex mappings from a low-resolution estimate  $\mathbf{H}_{LR}$  to the full-resolution channel response. The low-resolution input can be directly obtained from raw pilot observations ( $\mathbf{H}_{LR} = \mathbf{H}_p$ ) or constructed using traditional techniques such as LS combined with Linear Interpolation (LI), providing a less noisy but still incomplete representation of  $\mathbf{H}$ . This approach is analogous to SR techniques in image processing, where high-frequency details are recovered from degraded low-resolution inputs.

DL models such as ChannelNet [5] and EDSR [6] employ Convolutional Neural Networks (CNNs) to learn spatial patterns in the channel matrix, achieving improved estimation accuracy over classical methods. However, their high model complexity and computational cost hinder real-time deployment. In contrast, the Super Resolution Convolutional Neural Network (SRCNN) architecture [9] offers faster inference due to its shallow structure but suffers from reduced accuracy.

To improve the accuracy–efficiency trade-off, AttRNet [7] incorporates the lightweight SE mechanism [14] to emphasize relevant features while maintaining a compact model size. The LSidNN model [11] goes further by explicitly optimizing for low complexity, using a few dense layers to refine LS estimates, though this comes at the cost of reduced performance. On the other hand, CEViT [8] introduces a transformer-based architecture that leverages patch-wise self-attention to model long-range dependencies, achieving state-of-the-art accuracy, but at the expense of high computational complexity and inference latency. These trends highlight the need for a model that combines efficient local feature extraction, selective attention, and global context modeling, while maintaining low inference time, motivating the design of HELENA.

### III. HELENA ARCHITECTURE

HELENA is a lightweight DL model for pilot-based CE in 5G-NR OFDM systems, designed to balance accuracy and inference time. It combines convolutional feature extraction

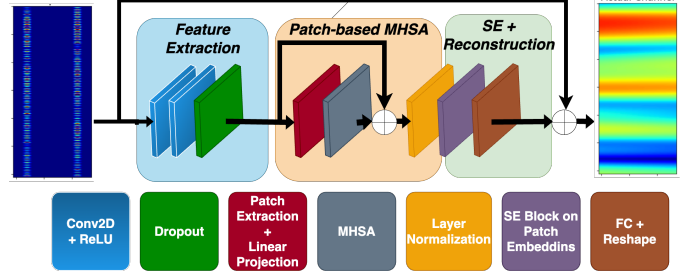


Fig. 1. The proposed HELENA architecture.

with dual attention: patch-wise MHSA for long-range context and a low-cost SE block for channel-wise recalibration. The input is a sparse LS-based estimate  $\mathbf{H}_{LR} \in \mathbb{R}^{N_S \times N_D \times 2}$ , where values are present only at pilot positions and set to zero elsewhere, while the output is a full-resolution estimate  $\hat{\mathbf{H}} \in \mathbb{R}^{N_S \times N_D \times 2}$  covering the entire time-frequency grid. The following subsection outlines the main architectural components and their design rationale.

#### A. Feature Extraction via Shallow CNN

To extract local spatial features from  $\mathbf{H}_{LR}$ , the model uses two 2D convolutional layers with ReLU activations. The first convolutional layer applies a kernel of size  $f_1 \times t_1$  and uses  $C_1$  filters, producing an intermediate feature map  $\mathbf{F}^{(1)}$ . The second layer uses a kernel of size  $f_2 \times t_2$  with  $C$  filters, resulting in  $\mathbf{F}^{(2)}$ . These layers have associated learnable weights  $\mathbf{W}_1, \mathbf{W}_2$  and biases  $\mathbf{b}_1, \mathbf{b}_2$ , respectively. A dropout layer is applied to improve generalization:

$$\mathbf{F}^{(1)} = \text{ReLU}(\text{Conv2D}_1(\mathbf{H}_{LR}; \mathbf{W}_1, \mathbf{b}_1))$$

$$\mathbf{F}^{(2)} = \text{ReLU}(\text{Conv2D}_2(\mathbf{F}^{(1)}; \mathbf{W}_2, \mathbf{b}_2))$$

$$\mathbf{F}_{\text{drop}} = \text{Dropout}(\mathbf{F}^{(2)})$$

The output tensor  $\mathbf{F}_{\text{drop}} \in \mathbb{R}^{N_S \times N_D \times C}$  is then partitioned into non-overlapping patches of height  $p$ , giving  $N = N_S/p$  patches. This patching strategy enables localized spatial aggregation while reducing the sequence length, making the subsequent attention computation more efficient. Each patch is then flattened into a vector:

$$\mathbf{F}_{\text{patch}}^{(i)} \in \mathbb{R}^{p \times N_D \times C}, \quad \mathbf{P}_i = \text{Flatten}(\mathbf{F}_{\text{patch}}^{(i)}) \quad (3)$$

#### B. Patch Embedding and Multi-Head Self-Attention

Each patch vector  $\mathbf{P}_i$  is projected into a shared  $d$ -dimensional embedding space using a learnable weight matrix  $\mathbf{W}_e \in \mathbb{R}^{(pN_D C) \times d}$  and bias  $\mathbf{b}_e \in \mathbb{R}^d$ :

$$\mathbf{Z}_i = \mathbf{P}_i \mathbf{W}_e + \mathbf{b}_e, \quad \mathbf{Z} \in \mathbb{R}^{N \times d} \quad (4)$$

Each flattened and embedded patch vector  $\mathbf{Z}_i$  represents a localized region of the input and is referred to as a *token*, following the terminology of transformer-based architectures. These  $N$  tokens are stacked to form the input matrix  $\mathbf{Z} \in \mathbb{R}^{N \times d}$ , where each row is a token embedding of dimension

$d$ . This token sequence is processed by the MHSA block to capture global context and long-range dependencies across the time-frequency grid. For each attention head  $j$ , the mechanism uses learnable projection matrices to map the input into a query  $\mathbf{Q}_j = \mathbf{Z}\mathbf{W}_j^Q$ , key  $\mathbf{K}_j = \mathbf{Z}\mathbf{W}_j^K$ , and value  $\mathbf{V}_j = \mathbf{Z}\mathbf{W}_j^V$ , where  $\mathbf{W}_j^Q, \mathbf{W}_j^K, \mathbf{W}_j^V \in \mathbb{R}^{d \times d_k}$  and  $d_k$  is the per-head dimension. The attention mechanism computes similarity between queries and keys to determine how much contextual information from each token (via the values) should be aggregated. The outputs from all  $h$  heads are concatenated and projected back using  $\mathbf{W}^O \in \mathbb{R}^{hd_k \times d}$  follow by a layer normalization mechanism. For further details, we refer to the original Transformer formulation [15].

$$\begin{aligned} \mathbf{Q}_j &= \mathbf{Z}\mathbf{W}_j^Q, \quad \mathbf{K}_j = \mathbf{Z}\mathbf{W}_j^K, \quad \mathbf{V}_j = \mathbf{Z}\mathbf{W}_j^V \\ \text{head}_j &= \text{Softmax} \left( \frac{\mathbf{Q}_j \mathbf{K}_j^T}{\sqrt{d_k}} \right) \mathbf{V}_j \\ \text{MHSA}(\mathbf{Z}) &= \text{Concat}(\text{head}_1, \dots, \text{head}_h) \mathbf{W}^O \\ \mathbf{Z}_{\text{att}} &= \text{LayerNorm}(\mathbf{Z} + \text{MHSA}(\mathbf{Z})) \end{aligned}$$

### C. Channel-wise Attention and Reconstruction

While MHSA captures long-range dependencies and aggregates contextual information across the full time-frequency grid, it treats all embedding channels equally during its output projection. However, not all channels (i.e., feature dimensions) contribute equally to the task of CE, e.g., some may carry more informative patterns depending on the propagation environment and pilot configuration. To recalibrate channel importance, HELENA applies a lightweight SE block [14] across the token embeddings. First, a global descriptor  $\mathbf{s} \in \mathbb{R}^d$  is computed via average pooling:

$$\mathbf{s} = \frac{1}{N} \sum_{i=1}^N \mathbf{Z}_{\text{att},i} \quad (5)$$

Then, two fully connected layers with weights  $\mathbf{W}_{\text{se1}} \in \mathbb{R}^{d \times d/r}$ ,  $\mathbf{W}_{\text{se2}} \in \mathbb{R}^{d/r \times d}$  and nonlinearities (ReLU and sigmoid) produce an scaled excitation vector  $\mathbf{e} \in \mathbb{R}^d$ :

$$\begin{aligned} \mathbf{e} &= \sigma(\mathbf{W}_{\text{se2}} \cdot \text{ReLU}(\mathbf{W}_{\text{se1}} \cdot \mathbf{s} + \mathbf{b}_{\text{se1}}) + \mathbf{b}_{\text{se2}}) \\ \mathbf{Z}_{\text{scaled},i} &= \mathbf{Z}_{\text{att},i} \odot \mathbf{e} \end{aligned}$$

This post-attention recalibration step enables the network to focus on semantically meaningful representations by learning a global importance weighting over the embedding dimensions and selectively amplify the most relevant features, all with minimal computational overhead. Then, each scaled token is projected back to the original patch space using reconstruction weights  $\mathbf{W}_r \in \mathbb{R}^{d \times (pN_D \cdot 2)}$  and bias  $\mathbf{b}_r \in \mathbb{R}^{pN_D \cdot 2}$ :

$$\mathbf{P}'_i = \mathbf{Z}_{\text{scaled},i} \mathbf{W}_r + \mathbf{b}_r \quad (6)$$

The set of projected patch vectors  $\{\mathbf{P}'_i\}_{i=1}^N$  is then reshaped and reassembled to form the output estimate  $\hat{\mathbf{H}} \in \mathbb{R}^{N_S \times N_D \times 2}$ :

$$\hat{\mathbf{H}} = \text{Reshape}(\{\mathbf{P}'_i\}_{i=1}^N) \quad (7)$$

TABLE I  
CHANNEL AND 5G-NR PARAMETERS FOR DATASET GENERATION

Parameter	Value/Description
Channel Profiles	TDL-A to TDL-E
Fading Distribution	Rayleigh
Antennas (Tx, Rx)	1, 1
Carrier Configuration	51 RB, 30 kHz SCS, Normal CP
Sub-carriers per Resource Block (RB)	12
Symbols per Slot	14
Slots per Subframe	2
Slots per Frame	20
Frame Duration	10 ms
NFFT	1024
Transmission Direction	Downlink
PDSCH Configuration	PRB: 0-50, All symbols, Type A, 1 layer
Modulation	16QAM
DM-RS Configuration	Ports: 0, Type A Position: 2 Length: 1, Config: 2
Delay Spread	1-300 ns
Doppler Shift	5-400 Hz
SNR	0-20 dB (2 dB steps)
Sample Rate	30.72 MHz
Noise	AWGN
Interpolation	Linear
Dataset Shape	[11264, 612, 14, 2] = [samples, SCS×RB, symbols, real & imaginary components]

Finally, a global residual connection [16] is included to improve convergence and ensure preservation of coarse structural information from the initial LS estimates [7], [17]:

$$\hat{\mathbf{H}} = \mathbf{H}_{\text{LR}} + \text{HELENA}(\mathbf{H}_{\text{LR}}) \quad (8)$$

The resulting DL architecture, HELENA (equivalent to  $f_{\Theta}$  in Eq. 2), combines local and global feature learning with low complexity. Its dual attention mechanism, MHSA and SE, enables accurate reconstruction without interpolation or side information, achieving high accuracy at low computational and memory cost as shown in Section IV.

## IV. EVALUATION RESULTS

### A. Dataset Description

The dataset was generated using MATLAB's 5G Deep Learning Data Synthesis code<sup>2</sup> with minor modifications. Key parameters, including Physical Downlink Shared Channel (PDSCH) configuration, central frequency, Subcarrier Spacing (SCS), Cyclic Prefix (CP) type, number of RBs, code rate, and modulation, are summarized in Table I. Compared to the original code, the SNR range was extended to 0-20 dB (11 values), with 1024 samples per value, totaling 11,264 samples split into 70% training, 15% validation, and 15% testing. Ground truth labels are derived from full CSI, while inputs differ by method: HELENA and LSIDNN use LS estimates at pilot positions; ChannelNet, EDSR, AttRNet, and CEViT use LI-interpolated LS estimates. The dataset includes 3GPP TDL-A to TDL-E profiles, various Doppler shifts, and SNR levels, enabling robust generalization across diverse 5G-NR propagation conditions.

### B. Baseline Methods, Models and Experimental Setup

We compare HELENA against seven DL-based baselines, SRCNN, ChannelNet [5], EDSR [6], AttRNet [7],

<sup>2</sup><https://nl.mathworks.com/help/5g/ug/deep-learning-data-synthesis-for-5g-channel-estimation.html>

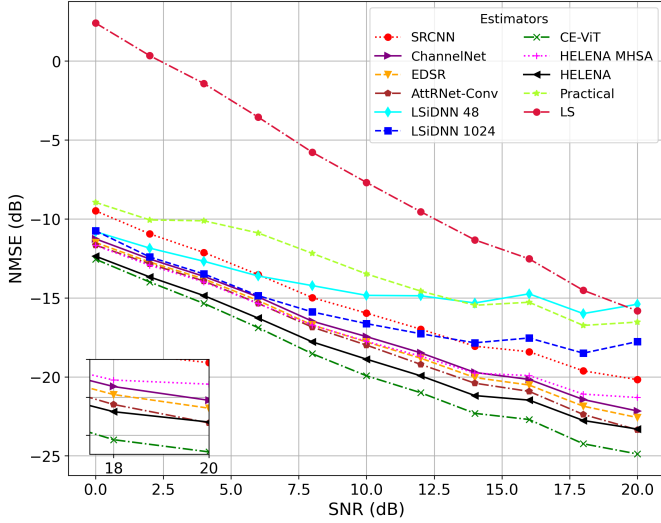


Fig. 2. NMSE vs. SNR for various CE methods.

TABLE II  
COMPARISON OF NMSE (dB), FLOPS, AND INFERENCE TIME USING  
HELENA AS BASELINE. LOWER VALUES ARE BETTER.

Model	Params ( $\times 10^6$ )	FLOPS ( $\times 10^9$ )	NMSE (dB)		Inference (ms)	
			Value	$\Delta$	Value	$\Delta$
SRCNN	0.014	0.241	-13.828	17.60%	0.120	-31.43%
ChannelNet	0.184	3.108	-15.507	7.59%	0.293	67.43%
EDSR	0.306	5.245	-15.773	6.03%	0.388	121.71%
AttNet-Conv	0.075	1.288	-15.993	4.70%	0.293	67.43%
LSiDNN 48	1.662	0.003	-13.546	19.28%	0.0738	-57.83%
LSiDNN 1024	35.11	0.070	-14.834	11.61%	0.158	-9.71%
CE-ViT	0.880	0.053	-17.303	-3.11%	0.318	81.71%
HELENA MHSA	0.114	0.072	-15.839	5.62%	0.172	-1.71%
HELENA	0.116	0.077	-16.782	—	0.175	—

LSiDNN [11], and CEViT [8], as well as two classical estimators: the LS method with LI, and a practical 5G-NR variant with denoising and averaging<sup>34</sup>.

All models were reimplemented with adaptations for deployment and fair comparison. ChannelNet uses 32 Denoising Convolutional Neural Network (DnCNN) filters (vs. 64). EDSR includes 32 filters and 16 residual blocks, restructured for joint I/Q input using 2D-CNNs. AttNet uses the AttNet-Conv variant (32 filters). LSiDNN is evaluated with 48 and 1024 neurons to reflect input size. CEViT uses Conv2DTranspose in place of inverse patch embedding for TensorRT compatibility. All models use `padding='same'` and omit upsampling. We also include HELENA-MHSA (without SE) to isolate the contribution of dual attention.

Experiments were run on the GPULab testbed<sup>5</sup> using 4 vCPUs, 64 GB RAM, and an NVIDIA Tesla V100-SXM3 (32 GB). The software stack included CUDA 12.2, TensorFlow 2.15, and TensorRT 8.6.1. Training used Adam optimizer and Mean Squared Error (MSE) loss (batch size 64), with

early stopping (patience 50) and learning rate 0.01, reduced by 0.8 every 40 epochs without improvement ( $\min 1 \times 10^{-5}$ ). Checkpoints were selected based on validation loss. Inference time was averaged over 100 single-sample runs. Results refer to TensorRT-optimized models, as non-optimized versions showed similar accuracy but are unsuitable for deployment [9].

### C. Design Decisions and Parameter Selection in HELENA

The parameters of HELENA were chosen based on the structural characteristics of the input data and validated empirically to optimize the trade-offs between estimation accuracy, inference time, and model complexity. The convolutional layers use  $12 \times 2$  and  $6 \times 7$  kernels to exploit the time-frequency layout of the OFDM grid while remaining lightweight. A patch size of 12 along the frequency axis yields 51 tokens, matching the 51 RBs in the dataset. Each token is embedded into a 64-dimensional space, which offers sufficient capacity for expressive representation while avoiding overfitting or excessive compute. The MHSA block uses 4 heads, allowing parallel modeling of diverse attention patterns without excessive overhead while maintaining high accuracy. A reduction ratio of 4 in the SE block avoids overly aggressive bottlenecking, enabling meaningful channel-wise recalibration at low cost. Dropout (rate 0.1) and residual connections further enhance generalization and convergence.

### D. Model Accuracy

Fig. 2 shows the Normalized Mean Squared Error (NMSE) across SNR. It is defined as

$$\text{NMSE} = \frac{\mathbb{E} [\|\hat{\mathbf{H}} - \mathbf{H}\|_2^2]}{\mathbb{E} [\|\mathbf{H}\|_2^2]}, \quad (9)$$

where  $\hat{\mathbf{H}}$  and  $\mathbf{H}$  denote the estimated and true channel matrices, respectively. NMSE is a standard metric in CE, as it provides a normalized, scale-invariant measure of estimation error and enables fair comparison across different SNR levels, channel conditions, and model complexities. Results are reported in dB to reflect performance on a logarithmic scale.

CEViT achieves the best NMSE ( $-17.303$  dB), followed closely by HELENA ( $-16.782$  dB), which requires no explicit SNR, Doppler, or latency inputs and avoids interpolation. Compared to LS ( $-3.56$  dB) and the practical estimator ( $-12.25$  dB), HELENA improves NMSE by 95.3% and 65.5%, respectively. Relative to other DL baselines, HELENA improves over EDSR ( $-15.773$  dB) by 6.03%, AttNet ( $-15.993$  dB) by 4.70%, and ChannelNet ( $-15.507$  dB) by 7.59%. Compared to SRCNN ( $-13.828$  dB), the gain reaches 17.60%. Removing the SE block reduces accuracy by 5.62%, confirming the benefit of the dual-attention design.

### E. Computational and Memory Cost vs. Inference Time

To meet the stringent latency requirements of 5G-NR, CE, equalization, and decoding must complete within the Hybrid Automatic Repeat Request (HARQ) deadline, which allows up to three Transmission Time Intervals (TTIs) (0.5 ms per TTI at 30 kHz SCS) [10]. This implies a tight budget of roughly

<sup>3</sup><https://www.mathworks.com/help/5g/ref/nrchannelestimate.html>

<sup>4</sup>[https://github.com/srsran/srsRAN\\_Project/blob/main/lib/phy/upper/signal\\_processors/port\\_channel\\_estimator\\_average\\_impl.cpp](https://github.com/srsran/srsRAN_Project/blob/main/lib/phy/upper/signal_processors/port_channel_estimator_average_impl.cpp)

<sup>5</sup><https://doc.ilabt.imec.be/ilabt/gpulab/>

0.5 ms for CE. As shown in Table II, all evaluated models satisfy this constraint.

HELENA achieves a strong trade-off: it delivers the second-best accuracy, just 3.1% lower than CEViT, and has the lowest inference time among the top-performing models (excluding HELENA MHSA). Specifically, CEViT and AttRNet are 81.71% (0.318 ms vs. 0.175 ms) and 67.43% (0.293 ms vs. 0.175 ms) slower, respectively. Compared to the lighter models, HELENA is 31.43% slower than SRCNN (0.120 ms) and LSiDNN-48 (0.0738 ms, 57.83% fastest) but they achieve it at the cost of higher prediction error. HELENA MHSA, which omits the SE block, performs nearly the same at 0.172 ms. All models complete within the 0.5 ms window, but HELENA uses only 35% of this budget, making it highly suitable for real-time deployment.

We can see that runtime does not scale linearly with computational complexity (in Floating-point operations per second (FLOPS)<sup>6</sup>). For example, HELENA uses 66.7% fewer FLOPS than SRCNN (0.08 vs. 0.24 G), yet runs 38.5% slower. AttRNet and EDSR require 16x and 65x more operations than HELENA, but inference is only 65.6% and 96.5% slower, respectively. ChannelNet also runs 37.9% slower, despite requiring 39x more FLOPS.

The number of parameters, which relates to the memory required at inference time, shows limited correlation with runtime or estimation accuracy. HELENA reaches  $-16.87$  dB NMSE with only 0.11M parameters, outperforming ChannelNet (0.18M) and LSiDNN-1024 (35.11M) while being faster. CEViT achieves the best NMSE with 0.88M parameters, 8x more than HELENA, but is slower. These results emphasize the need to jointly consider FLOPS, parameter count, and inference time when optimizing models for real-time CE, as actual latency is shaped by hardware–software co-design aspects such as memory access, operator fusion, and backend scheduling, which extend beyond theoretical complexity

## V. CONCLUSION

This letter presented HELENA, a DL-based model for efficient and accurate pilot-based CE in OFDM systems. HELENA combines shallow convolutional layers with dual attention, patch-wise MHSA and channel-wise SE, to balance estimation accuracy, model complexity, and inference time. Experimental results demonstrate that HELENA achieves near state-of-the-art accuracy with significantly fewer parameters and competitive runtime, making it well suited for real-time applications in latency-constrained systems such as 5G-NR. The observed weak correlation between FLOPS, parameter count, and inference time highlights the need for holistic evaluation criteria when designing DL-based CE models. Future work will extend HELENA to higher mobility scenarios, new waveform types, Multiple-Input Multiple-Output (MIMO) systems, and deployment on hardware platforms such as FPGA and edge AI accelerators. Furthermore, collecting real-world datasets and proposing standardized workflows for labeled channel data will be essential to validate performance and will

play a key role in enabling data-driven technologies such as Network Digital Twins (NDTs).

## ACKNOWLEDGMENTS

This research has been funded by the 6G-TWIN project, which has received funding from the Smart Networks and Services Joint Undertaking (SNS JU) under the EU's Horizon Europe research and innovation program under Grant Agreement No 101136314.

## REFERENCES

- [1] C. Qing, Z. Liu, G. Ling, W. Hu, and P. Du, "Channel estimation in ofds systems by leveraging differential modulation," *IEEE Transactions on Vehicular Technology*, vol. 74, no. 5, pp. 6907–6918, 2025.
- [2] C. Qing, W. Hu, Z. Liu, G. Ling, X. Cai, and P. Du, "Sensing-aided channel estimation in ofdm systems by leveraging communication echoes," *IEEE Internet of Things Journal*, vol. 11, no. 23, pp. 38 023–38 039, 2024.
- [3] J. Hoydis, F. A. Aoudia, A. Valcarce, and H. Viswanathan, "Toward a 6g ai-native air interface," *IEEE Communications Magazine*, vol. 59, no. 5, pp. 76–81, 2021.
- [4] M. Camelo, R. Mennes, A. Shahid, J. Struye, C. Donato, I. Jabandzic, S. Giannoulis, F. Mahfoudhi, P. Maddala, I. Seskar, I. Moerman, and S. Latre, "An ai-based incumbent protection system for collaborative intelligent radio networks," *IEEE Wireless Communications*, vol. 27, no. 5, pp. 16–23, 2020.
- [5] M. Soltani, V. Pourahmadi, A. Mirzaei, and H. Sheikhzadeh, "Deep learning-based channel estimation," *IEEE Communications Letters*, vol. 23, no. 4, pp. 652–655, 2019.
- [6] D. Maruyama, K. Kanai, and J. Katto, "Performance evaluations of channel estimation using deep-learning based super-resolution," in *2021 IEEE 18th Annual Consumer Communications and Networking Conference (CCNC)*, 2021, pp. 1–6.
- [7] W. Gao, W. Zhang, L. Liu, and M. Yang, "Deep residual learning with attention mechanism for ofdm channel estimation," *IEEE Wireless Communications Letters*, vol. 14, no. 2, pp. 250–254, 2025.
- [8] F. Liu, P. Jiang, J. Zhang, W. Wang, C.-K. Wen, and S. Jin, "Pd-cevit: A novel pilot pattern design and channel estimation network for ofdm systems," *IEEE Transactions on Communications*, pp. 1–1, 2024.
- [9] D. Göz, E. A. Beyazıt, N. Slamnik-Kriještorac, J. M. Marquez-Barja, N. Gaviria, S. Latré, and M. Camelo, "Computational efficiency of deep learning-based super resolution methods for 5g-nr channel estimation," in *2024 IEEE Latin-American Conference on Communications (LATIN-COM)*, 2024, pp. 1–7.
- [10] S. A. Damjanovic, E. Matus, D. Utyansky, P. van der Wolf, and G. P. Fettweis, "Channel estimation for advanced 5g/6g use cases on a vector digital signal processor," *IEEE Open Journal of Circuits and Systems*, vol. 2, pp. 265–277, 2021.
- [11] A. Sharma, S. A. U. Haq, and S. J. Darak, "Low complexity deep learning augmented wireless channel estimation for pilot-based ofdm on zynq system on chip," *IEEE Transactions on Circuits and Systems I: Regular Papers*, vol. 71, no. 5, pp. 2334–2347, 2024.
- [12] A. B. Singh and V. K. Gupta, "Performance evaluation of mmse and ls channel estimation in ofdm system," *International Journal of Engineering Trends and Technology (IJETT)*, vol. 15, no. 1, pp. 39–43, 2014.
- [13] J. Zhang, K. Qiu, Y. Li, H. Zhang, and M. Deng, "Channel estimation based on linear interpolation algorithm in ddo-ofdm system," in *Asia Communications and Photonics Conference and Exhibition*, 2010, pp. 605–606.
- [14] J. Hu, L. Shen, and G. Sun, "Squeeze-and-excitation networks," in *2018 IEEE/CVF Conference on Computer Vision and Pattern Recognition*, 2018, pp. 7132–7141.
- [15] A. Vaswani, N. Shazeer, N. Parmar, J. Uszkoreit, L. Jones, A. N. Gomez, L. Kaiser, and I. Polosukhin, "Attention is all you need," 2017. [Online]. Available: <https://arxiv.org/pdf/1706.03762.pdf>
- [16] K. He, X. Zhang, S. Ren, and J. Sun, "Deep residual learning for image recognition," in *Proceedings of the IEEE Conference on Computer Vision and Pattern Recognition (CVPR)*. IEEE, 2016, pp. 770–778. [Online]. Available: <https://arxiv.org/abs/1512.03385>
- [17] L. Li, H. Chen, H.-H. Chang, and L. Liu, "Deep residual learning meets ofdm channel estimation," *IEEE Wireless Communications Letters*, vol. 9, no. 5, pp. 615–618, 2019.

<sup>6</sup>Measured using TensorFlow's profiling tool: [https://www.tensorflow.org/api\\_docs/python/tf/compat/v1/profiler/ProfileOptionBuilder](https://www.tensorflow.org/api_docs/python/tf/compat/v1/profiler/ProfileOptionBuilder)